Available online at www.sciencedirect.com

SciVerse ScienceDirect

Journal of the European Ceramic Society 32 (2012) 905–913

www.elsevier.com/locate/jeurceramsoc

Magnetic properties of randomly oriented BaM, SrM, Co_2Y, Co_2Z and Co_2W hexagonal ferrite fibres

Robert C. Pullar [a,*], Igor K. Bdikin [b], Ashok K. Bhattacharya [c]

[a] *Dept. Engenharia Cerâmica e do Vidro/CICECO, Universidade de Aveiro, Campus Universitário de Santiago, 3810-193 Aveiro, Portugal*
[b] *Dept. Engenharia Mecânica, Universidade de Aveiro, Campus Universitário de Santiago, 3810-193 Aveiro, Portugal*
[c] *Department of Engineering Science, University of Oxford, Parks Road, Oxford OX1 3PJ, UK*

Received 16 June 2011; received in revised form 25 October 2011; accepted 29 October 2011
Available online 21 November 2011

Abstract

The microstructure and magnetic properties of randomly oriented $BaFe_{12}O_{19}$, $SrFe_{12}O_{19}$, $Ba_2Co_2Fe_{12}O_{22}$, $Ba_3Co_2Fe_{24}O_{41}$, $Ba_3Ca_{0.3}Co_2Fe_{24}O_{41}$ and $BaCo_2Fe_{16}O_{27}$ hexaferrite fibres were characterised. 2D and 3D AFM and MFM images were taken of a single BaM fibre. Magnetic properties of random ferrite fibres compared well to expected values for polycrystalline ceramics. The little-characterised Co_2W ferrite was found to have M_s and H_c similar to that of Co_2Z. Relatively small applied fields of <0.05 T were required to reverse the magnetisation of all the soft hexaplana ferrite fibres, and all had $H_c < 40$ kA/m, becoming demagnetised in fields <0.025 T. Random Co_2W fibres had a high M_r/M_s ratio of 0.56, (greater than M ferrites), despite being very magnetically soft (low coercivity), due to the unusual "lobed" shape of their hysteresis loop, which was attributed to their fibrous nature, and elongated growth of the grains along the fibre axis. Co_2Z had the lowest H_c of all the ferroxplana fibres.

Keywords: B. Fibres; B. Microstructure-final; C. Magnetic properties; D. Ferrites; Hexaferrites

1. Introduction

There exists a group of ferrites with a hexagonal crystal structure, known as the hexaferrites, that have become massively important materials commercially and technologically. Since their discovery in the 1950s[1] the degree of interest in them has grown enormously, and is still growing today. As well as their general magnetic properties, uses as magnetic recording and data storage materials, and a constant awareness of their microwave (MW) properties, there has been an explosion of interest in hexaferrites in the last decade for more exotic applications such as MW/GHz electronic components and EM absorbers (radar absorbing materials, RAM), as composite materials, magnetoelectric/multiferroic applications, and the development of hexaferrite fibres.

The hexagonal ferrites are all ferrimagnetic materials, and their magnetic properties are intrinsically linked to their crystalline structures. They all have magnetocrystalline anisotropy (MCA), that is, the induced magnetisation has a preferred orientation within the crystal structure, and they can be divided into two main groups.[2] Those with an easy axis of magnetisation, the uniaxial hexaferrites, have an MCA which is parallel to the *c*-axis, coming out of the basal plane of the hexagonal crystal. This uniaxial anisotropy in effect fixes the magnetisation in the direction of the *c*-axis, and the magnetisation can only be moved out of this direction at the expense of the high anisotropic energy. However, some compounds containing a divalent cation, especially those containing cobalt, can have an easy plane (or cone) of magnetisation, and were named the ferroxplana or hexaplana ferrites.[3] These compounds have spontaneous magnetisation either in the basal plane, perpendicular to the *c*-axis, or in a cone of magnetisation at an angle between 0 and 90° to the *c*-axis. While the direction of magnetisation can easily rotate within the plane or cone through an angle of 360°, the magnetisation is still locked in this plane or cone by a high magnetic anisotropy energy.[2]

The M ferrites, BaM ($BaFe_{12}O_{19}$) and SrM ($SrFe_{12}O_{19}$), are hard uniaxial ferrites, with high magnetic saturation (M_s) values and high coercivity (H_c).[1,2] The remnant magnetisation (M_r) is usually ~50% of the M_s value in randomly oriented M ferrites,

* Corresponding author. Tel.: +351 234 370 041.
E-mail address: rpullar@ua.pt (R.C. Pullar).

0955-2219/$ – see front matter © 2011 Elsevier Ltd. All rights reserved.
doi:10.1016/j.jeurceramsoc.2011.10.047

giving a ratio of M_r/M_s of 0.5. Co_2W ferrite ($BaCo_2Fe_{16}O_{27}$) has a cone of easy magnetisation at a constant angle of 70° to the *c*-axis from −273 °C to 180 °C, at which point this anisotropy rotates towards the *c*-axis with increasing temperature until it becomes uniaxial at 280 °C, and the magnetisation remains in the *c*-axis with a further rise in temperature.[4] Co_2Y ($Ba_2Co_2Fe_{12}O_{22}$) has cone of magnetisation below −58 °C, but above this temperature to the Curie point (i.e. including room temperature) it has a planar magnetic anisotropy.[3] Co_2Z ($Ba_3Co_2Fe_{24}O_{41}$) is planar at room temperature, but has a complex magnetic anisotropy, with at least four different anisotropic states. At low temperatures Co_2Z has an easy cone of magnetisation, at an angle of 65° to the *c*-axis, and this remains constant up to −103 °C. Between this temperature and −53 °C the angle increases to 90°, and the preferred magnetisation remains in the basal plane until it switches to the *c*-axis at some temperature between 207 and 242 °C.[2,5] The hexaplana ferrites are soft ferrites, with low H_c values, although they still have high M_s values. They usually have much lower M_r values, and ratio of $M_r/M_s \ll 0.5$. The structures of all the hexaferrites are very similar and constructed from three building blocks: simply put, taking the M, Y and S (spinel, $CoFe_2O_4$) phases as these building blocks, W = M + 2S and Z = M + Y.

It has been predicted that thermal, electrical, magnetic and optical properties could be enhanced in material in fibrous form. This is because a continuous fine fibre can be considered as effectively one-dimensional, and it does not behave as a homogeneously distributed powder or sintered monolith.[6] For this reason, there is great interest in composite materials containing hexaferrite fibres, and the synthesis of hexagonal ferrite fine ceramic fibres (<10 μm diameter) were first investigated by the authors. Pullar et al. reported a series of ferrites in the form of polycrystalline, continuous blow spun fibres produced rapidly and en-mass from a modified industrial process, not individually drawn metal wires or gel fibres pulled from a viscous gel. The random fibres so-produced are in the form of a random "wool-like" mass, they cannot be separated or produced individually, and are characterised only as a bulk product. Consequently, magnetostatic interaction between the fibres, misorientation of individual fibres, and shape anisotropy effects cannot be assessed for these materials, although work on magnetic microwires[7] has shown that significant differences may exist between the properties of individual fibres and blankets. Pullar et al. reported the synthesis of a range of random and aligned hexagonal ferrite fibres, including BaM and SrM,[8–11] Co_2Y,[12–14] Co_2Z[13,14] and Co_2W[15,13,14] hexaferrites, as well as haematite (α-Fe_2O_3) and magnetite (Fe_3O_4 spinel) fibres,[16] all blow spun from an aqueous inorganic sol–gel precursor. 0.67% CaO-doped Co_2Z fibres (Ca:Ba = 1:10) were also reported by the authors.[13] The fibres had diameters between 3 and 7 μm, and their microwave (GHz) ferromagnetic resonance characteristics were also reported.[17]

Since then other workers have made M ferrite fibres: BaM fibres with a diameter of 6 μm were made by an aqueous citrate gel method,[18] with organic spinning aids added, and 350 nm diameter solid and hollow BaM fibres were made by electrospinning, and then sintered at 700 °C.[19] SrM nanofibres have also been made by electrospinning, using poly(vinyl pyrrolidone) as a spinning aid, to produce random fibres.[20] Magnetic maghemite (γ-Fe_2O_3) solid fibres, hollow fibres, fibre-in tube and tube-in-tube nanostructures (<500 nm diameter) have been produced by electrospinning and annealing at 500 °C/2 h.[21] Song et al. published a series of articles in 2010 detailing the preparation of M ferrite hollow fibres drawn from a citrate gel to produce fibres of 1–4 μm diameter, and up to 10 cm length.[22–24] No one else seems to have reported fibres of the more complex hexaplana ferrites. In this paper we report and compare the magnetic properties of the random BaM, SrM, Co_2Y, Co_2Z and Co_2W hexaferrite fibres made by the authors. As the microstructure greatly affects the magnetic properties, we also characterise the microstructure of the random ferrite fibres.

2. Experimental

The fibres were blow spun from an aqueous halide-based sol–gel precursor, as described in the authors' previous publications.[8,9,12,13,15] In this case random gel fibres were collected, and fired in air between 700 and 1250 °C/3 h, at heating and cooling rates of 5 °C/min. The nitrate-based M ferrite fibres referred to for comparison are those measured previously by Pullar et al.[10] Scanning electron microscopy (SEM) was carried out on a Hitachi S-4100 at 10 kV on uncoated fibre samples. The fibres have already been shown to be single phase ferrites in previous publications.[14,25] To obtain the magnetic force microscopy (MFM) images, we used standard hard-magnetic tips (coercivity of ∼24 kA m^{-1} (300 Oe), force of 2.8 N m^{-1}, resonance frequency ∼75 kHz, PPP-MFMR, Nanosensors). The instrument was operated in combined tapping mode and lift mode with a tip-sample distance of 50–100 nm. Individual fibres were set in a polymer glue to hold them still for MFM analysis.

Magnetic measurements were taken on a Maglab Vibrating Sample Magnetometer (VSM) with a helium-cooled 12 T superconducting magnet, supplied by Oxford Research Instruments. The apparatus was controlled by six independent Oxford units, which were managed by, and the data collected using, Oxford Object Bench software. The sensitivity of the measurement was continuously maximised by an automatic phase sensitive detector lock-in amplifier. The hysteresis loops of the samples were measured in applied fields up to 5 T. Random fibre was ground lightly in a pestle and mortar, sufficient to produce a sample of discontinuous random fibres with an average length of approximately 100–200 μm, and an aspect ratio of at least 10. This was then weighed to ±0.05 mg and placed on a piece of tissue paper, soaked liberally with resin and allowed to dry, forming a flat sample that was slightly thicker in the centre, resembling a low square-based pyramid. The sample was then mounted on a PEEK sample holder and secured with PTFE tape, so that when inserted into the VSM the plane of the square would be parallel with the applied field. The details of this method have been reported previously.[26] It has also been demonstrated that the VSM can be accurately calibrated for measurement of such planar fibre samples with a 4 mm square made from a single layer of parallel lengths of pure nickel wire, with a diameter of 700 μm, set in resin as with the fibre samples. It was shown that, although there was a very slight shape effect upon M_s which varied with

Table 1
Comparison of magnetic characteristics of random hexagonal ferrite fibres at room temperature. All fibres were sintered at the stated temperature for 3 h. Nitrate-derived random BaM-NO_3 and SrM-NO_3 fibres have been reported previously by Pullar et al.[10]

Ferrite	Formula	Sintering temp. (°C)	M_s (A m^2 kg^{-1})	H_c (kA m^{-1})	M_r (A m^2 kg^{-1})	Isotropic M_r/M_s	Grain size (μm)
BaM	$BaFe_{12}O_{19}$	1000	63.8	420	30.9	0.48	0.3–1 μm
SrM	$SrFe_{12}O_{19}$	1000	63.3	455	31.3	0.49	0.3–1 μm
Co_2Y	$Ba_2Co_2Fe_{12}O_{22}$	1000	32.8	30	9.2	0.28	~2 μm
Co_2Z	$Ba_3Co_2Fe_{24}O_{41}$	1250	44.8	19	9.2	0.21	>10 μm
Ca-Co_2Z	$Ba_3Ca_{0.3}Fe_{24}O_{41}$	1200	45.7	25	11.5	0.25	~2 μm
Co_2W	$BaCo_2Fe_{16}O_{27}$	1250	44.2	39	24.7	0.56	>10 μm
BaM-NO_3	$BaFe_{12}O_{19}$	750	58.4	401	30.0	0.51	<0.1 μm
SrM-NO_3	$SrFe_{12}O_{19}$	700	65.0	440	32.7	0.50	<0.1 μm

alignment, the shape demagnetisation due to the sample being in the form of a flat square were negligible, and calibration of the VSM was reliable.[27] Unless otherwise stated, the measurements were taken at 300 K.

3. Results and discussion

The firing temperatures used for the random hexaferrite fibres reported in this article are shown in Table 1, along with their grain sizes and summaries of their magnetic properties. The nitrate-based sol–gel M ferrite random fibres reported previously by the authors are included for comparison. From X-ray diffraction (XRD) data previously published,[8,9,12,13,14,15] the fibres appeared to be the single phase of each hexaferrite at the temperatures shown in Table 1, within the limits of XRD detection of secondary phases, and allowing for the complex nature and high degree of similarity between the hexagonal ferrites. X-ray fluorescence (XRF) elemental analysis confirmed the stoichiometric composition of the M ferrite fibres as $Ba_{0.96}Fe_{12}O_{18.96}$ and $Sr_{0.98}Fe_{12}O_{18.98}$,[14] and the XRF compositions of the Co_2Y and Co_2W ferrites were similarly close to ideal stoichiometry,[12,15] and well within the limits of error of this technique. The XRF composition of Co_2Z fibres varied between $Ba_{2.93}Co_{1.85}Fe_{24}O_{40.78}$ and $Ba_{2.79}Co_{2.07}Fe_{24}O_{41.86}$, which is still very close to the ideal pure phase stoichiometry.[14] Ferromagnetic resonance measurements (FMR) also gave resonant peaks at the expected frequencies for pure phase materials at 43.5 GHz, 50 GHz and 1.3 GHz for BaM, SrM and Co_2Z respectively,[9,13] and little or no discernible FMR peaks for Co_2Y and Co_2W.[17]

3.1. BaM random fibres

As can be seen in the SEM images in Fig. 1(a), the BaM random fibres were around 4–5 μm diameter when fired at 1000 °C. They consisted of mostly submicron grains between 300 nm and 1 μm in diameter and 200–300 nm thick, with either a poorly hexagonal or irregular polygonal shape. A few large pores in the order of 100–200 nm could also be observed between the grains. The estimated porosity reported previously from surface area measurements of these BaM fibres gave a low surface area of 0.86 m^2 g^{-1}, a low pore volume of 0.004 cm^3 g^{-1} (=~2% porous) and a calculated average pore diameter of 53 nm.[14] Although the observed intergranular pores appear larger than this, the value of ~2% porosity reported earlier generally agrees with the degree of porosity seen here. Topographical AFM images of a BaM fibre set in a polymer glue are shown in Fig. 2(a), along with 3D renders from these images in Fig. 2(b). The grains can clearly be seen in the images, and both their sizes (≤1 μm) and the fibre diameter agree with the SEM data. Fig. 2(c) shows a 3D image of a BaM fibre, with detailed views of the area within the square showing AFM topography (Fig. 2(d)), MFM phase showing magnetic domains (Fig. 2(e)) and dz/dx 2D image of the physical grain structure (Fig. 2(f)), all on the same area of sample. The MFM image confirms that the magnetic domains are randomly oriented and submicron in size.

The uniaxial nature of BaM gives a large theoretical maximum coercivity of 594 kA m^{-1}, although the reported H_c values for BaM prepared from standard ceramic methods are much lower, and the maximum magnetisation of BaM is 72 A m^2 kg^{-1},[2] but polycrystalline samples rarely approach these high values. The random BaM fibres had M_s = 63.8 A m^2 kg^{-1} (Fig. 3(a)), and were very hard ferrites with H_c = 420 kA m^{-1} and M_r = 30.9 A m^2 kg^{-1}, giving a ratio of M_r/M_s of 0.48 (Fig. 3(b)). This compares well with other polycrystalline BaM ferrites made by various methods, and the low M_r/M_s ratio demonstrates that the individual magnetic domains are not oriented.

The BaM random fibres reported previously by Pullar et al. from a halide free, nitrate-based sol–gel precursor formed the single phase M ferrite at much lower temperatures of 750 °C/h.[10] It has been shown that this is due to a retardation effect of the halides, in particular chloride ions, on hexaferrite formation, delaying the pure M phase ferrite until firing temperatures of 1000 °C, at which point the halide is all removed.[14] As the nitrate-based BaM formed at a lower temperature, the grains were much smaller, and none were visible at all on SEM images, suggesting they were <100 nm in diameter, and resulting in very smooth looking fibres. However, despite this, the magnetic properties were broadly similar, with slightly lower values of M_s = 58.4 A m^2 g^{-1}, H_c = 401 kA m^{-1}, and M_r/M_s = 0.51.

3.2. SrM random fibres

The SEM images in Fig. 1(b) show that, although on the macroscale they seem very similar to the BaM fibres, the

microstructure of the SrM fibres is subtly different. The SrM random fibres were ~6 μm diameter when fired at 1000 °C, and although the grains exhibited a similar range of diameters ≤1 μm, there appeared to be more micron-sized grains. These SrM grains were also much more clearly defined hexagonal plates, and were more planar looking, even though they had similar thicknesses to the BaM grains of 200–300 nm. The intergranular pores were of a similar size, but if anything these fibres appeared slightly more porous, and the calculated porosity from shrinkage was estimated to be higher for SrM than BaM fibres.[14] The saturation magnetisation of single crystal SrM has been reported as 74.3 A m^2 kg^{-1},[28] and the maximum coercivity as 533 kA m^{-1},[29] but polycrystalline samples rarely approach these high values. These random SrM fibres had M_s = 63.3 A m^2 kg^{-1} (Fig. 3(a)), and were very hard ferrites with H_c = 455 kA m^{-1} and M_r = 31.3 A m^2 kg^{-1}, giving a ratio of M_r/M_s of 0.49 (Fig. 3(b)).

Similarly to BaM, the SrM random fibres reported previously by the authors from a halide free, nitrate-based sol–gel precursor formed the single phase M ferrite at an even lower temperature of 700 °C/h.[10] This resulted in very smooth looking fibres with much smaller grains < 100 nm in diameter, but in this case with slightly higher magnetisation of M_s = 65.0 A m^2 g^{-1}, H_c = 440 kA m^{-1}, and M_r/M_s = 0.50.

3.3. Co_2Y random fibres

The Co_2Y fibres fired to 1000 °C were between 6 and 7 μm diameter, consisting mostly of very-obviously-platy grains. The plates can appear to be needles when viewed edge-on in SEM

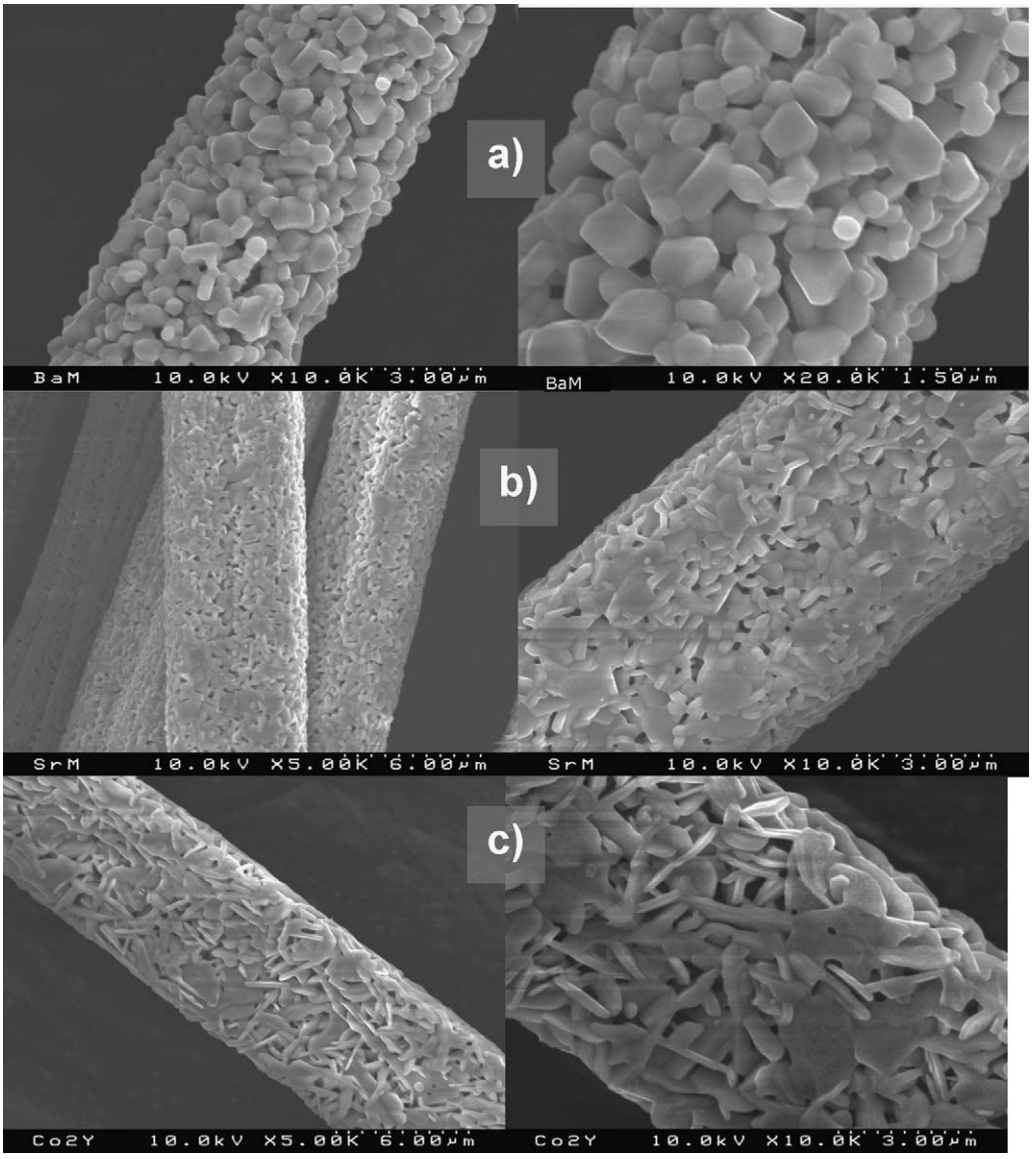

Fig. 1. SEM images of random hexaferrite fibres. (a) BaM fibres, fired at 1000 °C/3 h; (b) SrM fibres, fired at 1000 °C/3 h; (c) Co_2Y fibres, fired at 1000 °C/3 h; (d) Co_2Z fired at 1000 °C/3 h; (e) Co_2Z fired at 1200 °C/3 h; (f) Co_2Z fired at 1250 °C/3 h; (g) 0.67% CaO-doped Co_2Z fired at 1200 °C/3 h; and (h) Co_2W fibres, fired at 1250 °C/3 h.

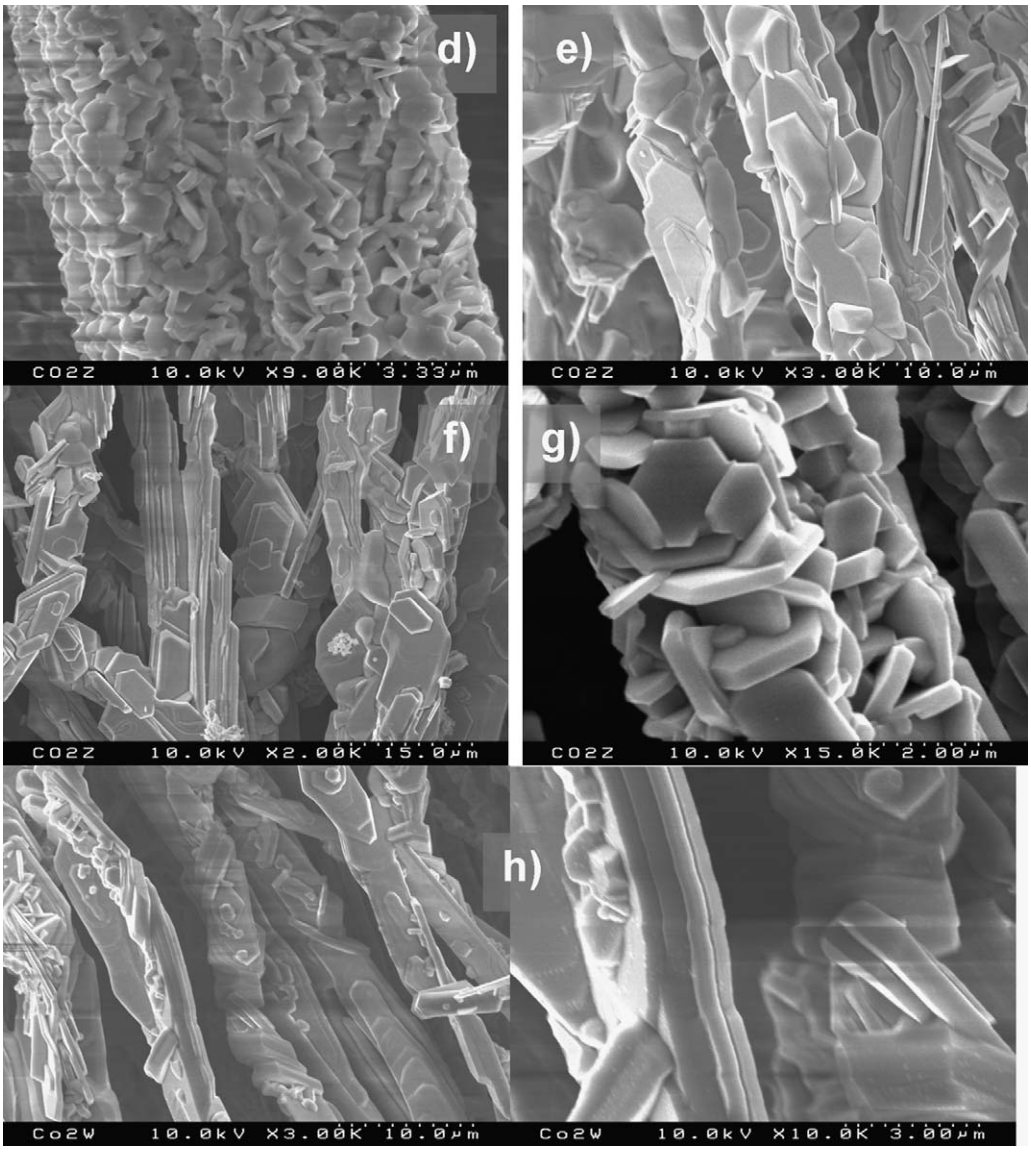

Fig. 1. (*Continued*).

images, but they are clearly thin plates, as can be observed from grains seen at a low angle (Fig. 1(c)). The plates seemed less obviously hexagonal than those seen in other hexaferrite fibres, with a more irregular shape, but they were wider and thinner than the M ferrites, with an average diameter of ~2 μm and a thickness of 100–200 nm. A greater degree of intergranular porosity was also evident than that of the M ferrite fibres. Co_2Y had the lowest M_s value of all the ferrite fibres of 32.8 A m^2 kg^{-1} at 3 T (Fig. 3(a)), which compared well to the maximum reported value of 34 A m^2 kg^{-1}.[2] It was a very soft ferrite, with H_c = 30 kA m^{-1}, M_r = 9.2 kA m^2 kg^{-1} (M_r/M_s = 0.28, Fig. 3) and a regularly shaped loop around zero field with no narrowing or lobing (Fig. 3(c)).

3.4. Co_2Z random fibres

Barium Co_2Z ferrite never forms directly from the mixed oxides, and the BaM and Co_2Y phases always have to co-exist first. It is suggested that these react and stack in alternate layers to form the Co_2Z structure (which is equivalent to M + Y ferrite), in a topotactic reaction.[30] At 1000 °C, the stoichiometric Co_2Z fibres actually consisted of a mixture of BaM and Co_2Y phases, with a structure resembling that of the Co_2Y fibres, but with smaller platy hexagonal grains about 1 μm in diameter and 50 nm thick (Fig. 1(d)). As can be seen in Fig. 3(a) and (b), this mixture of M and Y phases resulted in a hard ferrite fibre with a sizable H_c of 243.5 kA m^{-1}, which was between that of the respective BaM and Co_2Y phases seen in Sections 3.1 and 3.3. M_s at 4 T was closer to the M ferrite values at 58.7 A m^2 kg^{-1}, and M_r was 25.2 A m^2 kg^{-1}, giving a ratio of M_r/M_s = 0.43, less than that of BaM.

At 1200 °C, the Z phase had started to form, and DGG had initiated, resulting in some extremely elongated hexagonal plates over 10 μm long, but only 300–500 nm thick, stretching along the fibre axis (Fig. 1(e)). DGG always seems to be associated with the formation of the Co_2Z phase in polycrystalline

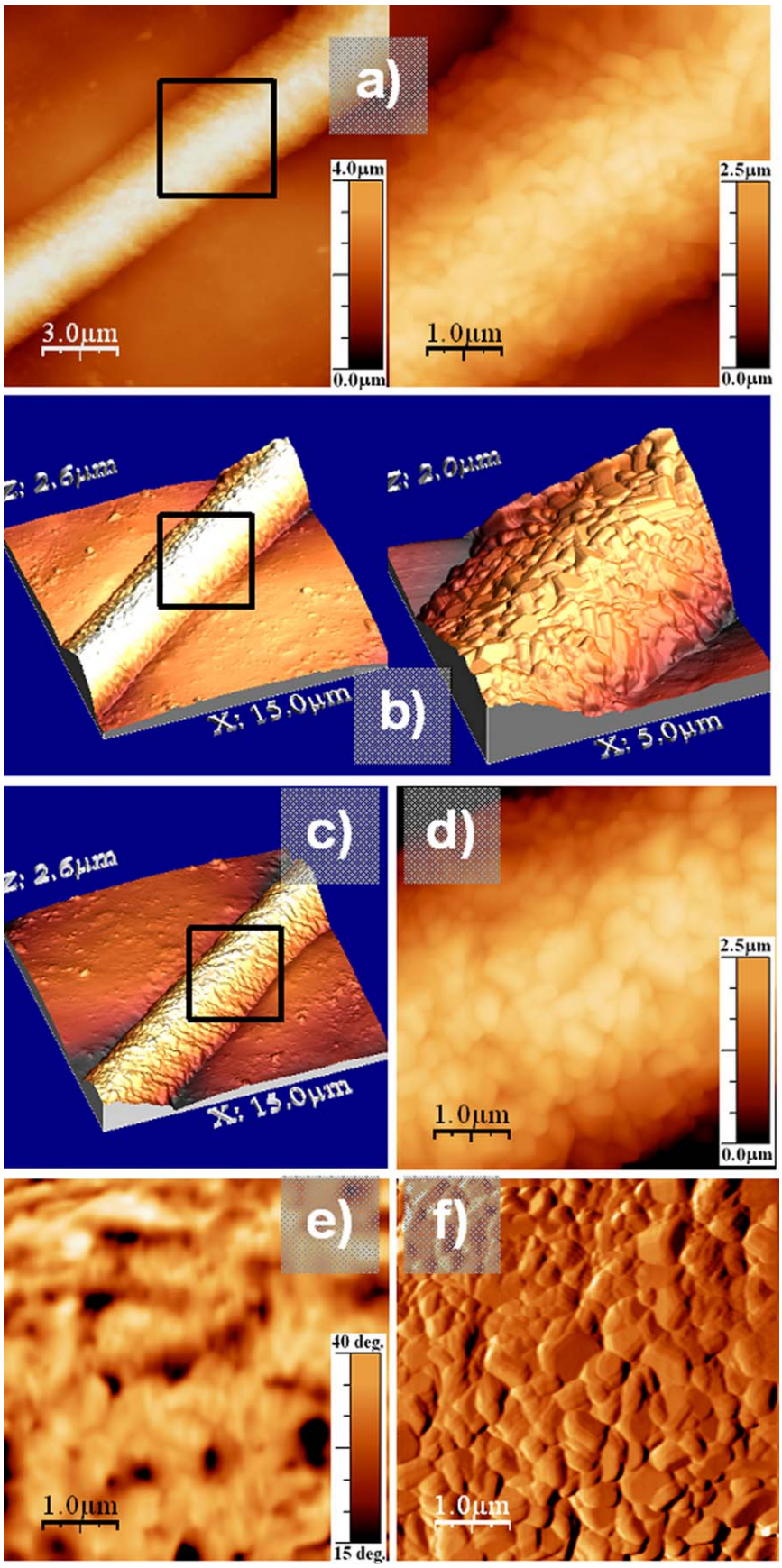

Fig. 2. AFM topography images (a) and rendered 3D images (b) of the same areas of a single BaM fibre, showing grain structure. (c) Rendered 3D AFM image of a BaM fibre, with an enlarged view of the area within the square showing (d) AFM topography; (e) MFM phase showing magnetic domains; and (f) *dz*/*dx* 2D image of physical grain structure.

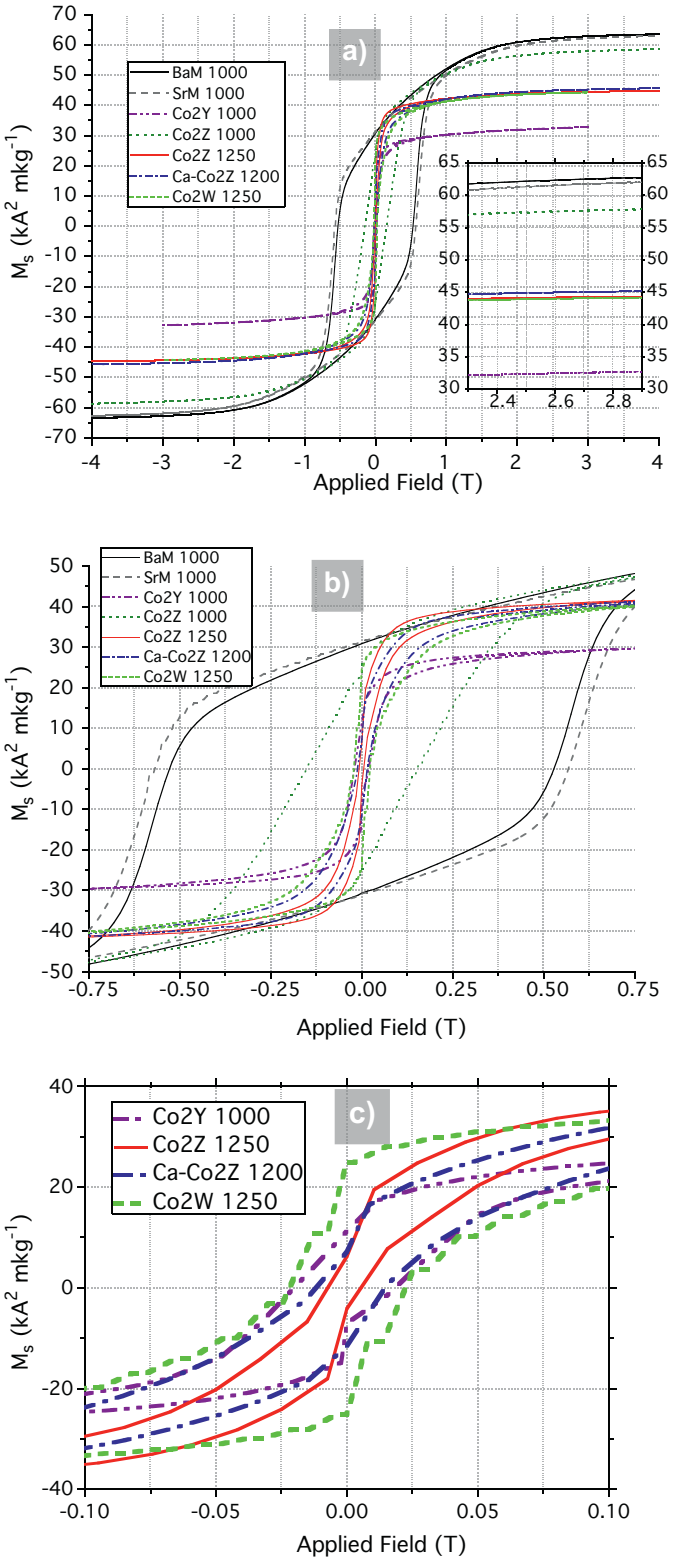

Fig. 3. (a) Magnetic hysteresis loops of random hexaferrite fibres – insert shows detail of near-maximum M_s values for all fibres around 3 T. (b) Detail of the magnetic hysteresis loops of random hexaferrite fibres with an applied field up to 0.75 T, to compare the loop shapes, and H_c and M_r values. (c) Expanded view to show the narrow magnetic hysteresis loops of random ferroxplana soft ferrite fibres with an applied field up to 0.1 T.

ceramics. By 1250 °C the fibres were single phase Co_2Z, and virtually all of the grains had undergone DGG, resulting in fibres that resembled rows of roofing slates or fallen dominoes in appearance. It can clearly be seen from the SEM images that the long, platy DGG associated with Z formation had occurred, with a quite different morphology to the pure Co_2Y or mixed Co_2Y–BaM fibres in Fig. 1(c) and (d). Some of the smaller grains still showed a hexagonal character, but most were very elongated, and the stacking of layers could clearly be observed on the surfaces of the grains (Fig. 1(f)). The resultant fibres were mechanically fragile, but remained as discrete individual fibres when viewed at low magnification.[13] When fired at 1250 °C/3 h, M_s was still high at 44.8 A m^2 kg^{-1} at 4 T (Fig. 3(a)), compared to maximum values of ~50 A m^2 kg^{-1} previously reported for Co_2Z ceramics.[2] However, the Co_2Z fibres were extremely magnetically soft, with a very narrow loop of H_c = 19 kA m^{-1}, and a low M_r of 9.2 A m^2 kg^{-1}, giving a ratio of M_r/M_s = 0.21 (Fig. 3(b)).

The presence of any BaM at all, even in small quantities, would result in a much wider loop, and the presence of a significant amount of Y ferrite would result in a lowered M_s value. It is possible that a very small amount of the W phase is present, as it is a decomposition product of Co_2Z, but if present it is in such small levels that it cannot be detected by XRD, and has not significantly affected the magnetic or FMR properties of the Z ferrite. When the hysteresis loop was examined in more detail around zero field (Fig. 3(c)), it could be seen that Co_2Z had the lowest H_c of all the ferroxplana fibres, with a narrowing of the loop around 0 T not seen in the Co_2Y ferrite, and that M_s increased more rapidly with an applied magnetic bias at low field values < 0.1 T compared to the other soft ferroxplana ferrites. The very slight widening of the loop just above and below zero H is a very small feature, a deviation only observed between 0 and 0.05 T (<500 G), and resulting in a tiny change in values. The low M_r value at 0 T is unaffected by this slight widening effect at very low applied fields. The possibility of coexistence and similarity of crystal structure makes it very difficult to say with absolute certainty that the hexaplana ferrites are absolutely pure single phase materials, but all the evidence suggests that this is Z ferrite, and that any slight lobing may be an effect of the fibrous nature of these samples, as is discussed in more detail in Section 3.5.

In 0.67 wt% CaO-doped Co_2Z fibre (equivalent to $Ba_3Ca_{0.3}Co_2Z$), the addition of Ca^{2+} was shown to reduce the formation temperature of the Z phase to ~1150 °C, resulting in an improved morphology with more equiaxed grains and no DGG up to 1200 °C. This was suggested to be due to the segregation of Ca^{2+} at the grain boundaries slowing the rate of grain growth in the hexagonal plane,[13] allowing growth to proceed in the direction of the c-axis as well. At 1200 °C the 0.67% CaO-doped Co_2Z fibre consisted of regular hexagonal grains up to 2 μm diameter and 300 nm thick (Fig. 1(g)). The microwave properties of the CaO-doped Z fibres fired to 1200 °C/3 h were clearly inferior to those of pure Co_2Z fired to 1250 °C/3 h,[17] but there was much less difference in their magnetic hysteresis loops. Ca-doped Co_2Z at 1200 °C had slightly higher values, with M_s = 45.7 A m^2 kg^{-1} (Fig. 3a)), H_c = 24.7 kA m^{-1}

and $M_r = 11.5\ A\ m^2\ kg^{-1}$ ($M_r/M_s = 0.25$, Fig. 3(b)). Although still a very soft ferrite, the loop did not narrow so obviously around 0 T, and hence M_s did not increase as rapidly as for pure Co_2Z at very low applied fields (Fig. 3(c)).

3.5. Co_2W random fibres

By the time they had become single phase Co_2W at 1250 °C, DGG had occurred in the Co_2W fibres, resulting in distorted plates stacked in layers four- or five-high, resembling geological strata (Fig. 1(h)). The individual platelets were as wide as the whole width of the fibre (3–4 μm wide), and could be up to tens of microns in length, but a uniform 0.5 μm thick, and were even more elongated along the fibre length than the Co_2Z fibres. The larger elongated plates had lost their hexagonal character, but this could still be seen in the smaller plates, and there was much evidence of one layer growing on top of another. Although on a macroscale they retained their fibrous nature, the individual fibres were very weak and brittle due to their crystalline morphology.

Co_2W ferrite has been much less reported than the other ferrites here, and there are few detailed hysteresis loops published for comparison. It is known to be a soft ferrite, usually with H_c slightly greater than Co_2Z, and M_s ~50 $A\ m^2\ g^{-1}$.[2] When fired to 1250 °C/3 h, M_s of the Co_2W fibres was similar to that of the Z ferrite fibres at 44.2 $A\ m^2\ kg^{-1}$ (Fig. 3(a)), and Co_2W was still a very soft ferrite with $H_c = 39\ kA\ m^{-1}$. However, when the loop was examined in more detail at low fields (Fig. 3(c)), it could be seen that it had a much higher M_r of 24.7 $A\ m^2\ kg^{-1}$, equivalent to a M_r/M_s ratio of 0.56, even higher than that of the M ferrite fibres, despite this being a very soft magnet with a low coercivity. This was due to the unusual shape of the Co_2W loop, which maintained a higher M_r value at 0 T, but then underwent a rapid decrease in magnetisation with a small applied opposite magnetic bias to give a low H_c. This resulted in a very non-linear "lobed" appearance around zero field for Co_2W. The precursor phases to Co_2W are BaM and $CoFe_2O_4$ spinel, both of which would result in greatly increased H_c values at zero field if present (like the Co_2Z at 1000 °C), and it decomposes into $BaFe_2O_4$, which is non magnetic. The Co_2Y and Co_2Z phases reported here have smaller H_c and M_r values, and would not explain the increased lobing if they were impurities in Co_2W. The M_s value and lack of any FMR peak suggest that this is pure W phase, and we attribute the strange loop shape to the unique fibrous nature of the sample, being even greater in this case than for the Co_2Z fibres due to the extreme elongated grain growth along the fibre axis.

Unpublished work by the authors on aligned Z and W ferrite fibres also shows that the lobing effect is much less apparent in Z than W ferrites, and that it is enhanced in both W and Z fibres when the aligned fibres are oriented parallel to the magnetic field, compared to when they are perpendicular to the field. It can be seen in Fig. 1(f) and (h) that under DGG the grains elongate along the fibre axis in Co_2W and Co_2Z ferrites, and to a greater extent in the W ferrite. We suggest that this lobing effect is at least partly due to the unique fibrous nature of these samples, not intrinsic to all Co_2W ceramics, and it is observed to a greater effect when these crystals become more elongated or deformed along the fibre axis. Similar effects have also been reported in $ZnFe_2O_4$ nanowires.[31] Variations in M_s with orientation have been observed and reported for aligned M ferrite fibres by the authors,[27] and although this effect was reduced when oriented perpendicular to the fibre, when oriented at 45° to the field the effect was similar to that when parallel with the field. Therefore, it makes sense that in a randomly aligned fibre, a strong, net-fibre-effect should be seen due to this elongation along the fibre length. Further evidence to support this is the fact that this lobing effect is not observed in the Co_2Y or CaO-doped Co_2Z fibres, which do not have the massively elongated grains along the fibre axis (Fig. 1(c) and (g)).

4. Conclusions

The microstructures of the various ferrite fibres were examined by SEM, and the grain size was seen to be up to 1 μm for the M ferrites, 1–2 μm for the Co_2Y and 0.67% CaO-doped Co_2Z ferrites, and over 10 μm for the Co_2Z and Co_2W ferrites. AFM images were taken of a single BaM fibre, and 3D renders of the AFM image confirmed the fibre diameter and microstructure observed by SEM. MFM images showed a randomly oriented magnetic sub-micron domain structure in BaM fibres.

The magnetic properties of the random ferrite fibres are summarised in Table 1, and compared well to the expected values for polycrystalline ceramics. The M ferrites (and the Co_2Z precursor fibre at 1000 °C) were hard ferrites, while the ferroxplana ferrites were all very soft ferrites. The little-characterised Co_2W ferrite was found to have M_s similar to that of Co_2Z, and a slightly larger H_c. Relatively small applied fields of only 0.05 T (500 G) were required to more-or-less fully reverse the magnetisation of all the soft hexaplana ferrite fibres, and all had an $H_c < 40\ kA\ m^{-1}$, becoming demagnetised in fields under 0.025 T. This makes them ideal for microwave devices, security, switching and sensing applications, and such low fields are easily achievable with small permanent magnets or low power electromagnets. Interestingly, the Co_2W ferrite fibres had a surprisingly high M_r of ~25 $A\ m^2\ g^{-1}$, resulting in a M_r/M_s ratio of 0.56, even higher than that of the M ferrite fibres, despite this being a very soft magnet with a low coercivity. This was due to the unusual "lobed" shape of the hysteresis loop of the Co_2W ferrite fibres, with a rapid decrease in M_s occurring only once a reverse magnetic bias was applied. Co_2Z had the lowest H_c of all the ferroxplana fibres, with a narrowing of the loop around 0 T not seen in the others, and M_s increased more rapidly with an applied magnetic bias at low field values < 0.1 T, compared to the other soft ferroxplana ferrites.

This lobed loop shape could possibly be due to the influence of a tiny amount of an undetected secondary magnetic phase, but it was observed in many different variations and syntheses of Co_2W and Co_2Z ferrites and fibres made by the authors. It was attributed to the fibrous nature of the samples, and the fact that in Co_2W, and to a lesser extent Co_2Z, DGG results in greatly elongated grain growth along the fibre axis. Only the Co_2Z and Co_2W ferrite fibres really exhibited any significant degree of

lobing, and the fact that this lobing was not seen in the CaO-Co_2Z and Co_2Y fibres, which although similar soft hexaplana ferrites, did not have this elongated DGG along the fibre length, supports this. Therefore, we are suggesting that this effect is due to the fibrous nature of these samples, specifically the elongated DGG which occurs along the fibre length in the Co_2W and Co_2Z fibres. We expect this effect to be more apparent in aligned fibres.

Acknowledgement

R.C. Pullar and I.G. Bdikin would like to thank the FCT Ciência 2008 programme for supporting this work.

References

1. Went JJ, Rathenau GW, Gorter EW, Van Oosterhout GW. Hexagonal iron-oxide compounds as permanent-magnet materials. *Phys Rev* 1952;**86**:424–5.
2. Smit J, Wijn HPJ. *Ferrites*. Eindhoven: Philips Technical Library; 1959.
3. Jonker GH, Wijn HPJ, Braun PB. Ferroxplana, hexagonal ferromagnetic iron-oxide compounds for very high frequencies. *Phil Tech Rev* 1956;**18**:145–80.
4. Samaras D, Collomb A, Hadjivasiliou S, Achilleos C, Tsoukala J, Pannetier J, et al. The rotation of the magnetization in the $BaCo_2Fe_{16}O_{27}$ W-type hexagonal ferrite. *J Magn Magn Mater* 1989;**79**:193–201.
5. Albanese G, Deriu A, Rinaldi S. Sublattice magnetization and anisotropy properties of $Ba_3Co_2Fe_{24}O_{41}$ hexagonal ferrite. *J Phys C* 1976;**7**:1313.
6. Hale DK. The physical properties of composite materials. *J Mater Sci* 1976;**11**:2105–41.
7. Gawronski P, Zhukova V, Blanco JM, Kulakowski K. Dynamics of interacting wires. *J Magn Magn Mater* 2002;**249**:9–15.
8. Pullar RC, Taylor MD, Bhattacharya AK. Novel aqueous sol–gel preparation and characterisation of barium M ferrite, $BaFe_{12}O_{19}$ fibres. *J Mater Sci* 1997;**32**:349–52.
9. Pullar RC, Appleton SG, Bhattacharya AK. The manufacture, characterisation and microwave properties of aligned M ferrite fibres. *J Magn Magn Mater* 1998;**186**:326–32.
10. Pullar RC, Taylor MD, Bhattacharya AK. A halide free route to the manufacture of microstructurally improved M ferrite ($BaFe_{12}O_{19}$ & $SrFe_{12}O_{19}$) fibres. *J Eur Ceram Soc* 2002;**22**:2039–45.
11. Pullar RC, Taylor MD, Bhattacharya AK. Halide removal from BaM ($BaFe_{12}O_{19}$) and SrM ($SrFe_{12}O_{19}$) ferrite fibres via a steaming process. *J Mater Res* 2001;**16**:3162–9.
12. Pullar RC, Taylor MD, Bhattacharya AK. Magnetic Co_2Y ferrite, $Ba_2Co_2Fe_{12}O_{22}$ fibres produced by a blow spun process. *J Mater Sci* 1997;**32**:365–8.
13. Pullar RC, Appleton SG, Stacey MH, Taylor MD, Bhattacharya AK. The synthesis and characterisation of aligned fibres of the ferroxplana ferrites Co_2Z, 0. 67% CaO-doped Co_2Z, Co_2Y and Co_2W. *J Magn Magn Mater* 1998;**186**:313–25.
14. Pullar RC, Stacey MH, Taylor MD, Bhattacharya AK. Decomposition, shrinkage and evolution with temperature of aligned hexagonal ferrite fibres. *Acta Mater* 2001;**49**:4241–50.
15. Pullar RC, Taylor MD, Bhattacharya AK. Aligned hexagonal Co_2W ferrite fibres, $BaCo_2Fe_{16}O_{27}$ produced from an aqueous sol–gel process. *J Mater Sci* 1997;**32**:873–7.
16. Pullar RC, Pyke DR, Taylor MD, Bhattacharya AK. The manufacture and characterisation of single phase magnetite and haematite aligned fibres from an aqueous sol–gel process. *J Mater Sci* 1998;**33**:5229–35.
17. Pullar RC, Appleton SG, Bhattacharya AK. The microwave properties of aligned hexagonal ferrite fibers. *J Mater Sci Lett* 1998;**17**:973–5.
18. Gong CR, Fan GL, Song CL, Lu G. Preparation and characterization of m-type barium ferrite fibers via aqueous sol–gel process. *Trans Tianjin Univ* 2007;**13**:117–20.
19. Mou F-Z, Guan J-G, Sun Z-G, Fan X-A, Tong G-X. In situ generated dense shell-engaged Ostwald ripening: a facile controlled-preparation for $BaFe_{12}O_{19}$ hierarchical hollow fiber arrays. *J Solid State Chem* 2010;**183**:736–43.
20. Shen X, Liu M, Song F, Meng X. Structural evolution and magnetic properties of $SrFe_{12}O_{19}$ nanofibers by electrospinning. *J Sol-Gel Sci Technol* 2010;**53**:448–53.
21. Mou F, Guan J, Shi W, Sun Z, Wang S. Oriented contraction: a facile nonequilibrium heat-treatment approach for fabrication of maghemite fiber-in-tube and tube-in-tube nanostructures. *Langmuir* 2010;**26**: 15580–5.
22. Song F, Shen X, Liu M, Xiang J. Formation and characterization of magnetic barium ferrite hollow fibers with high specific surface area via sol–gel process. *Solid State Sci* 2010;**12**:1603–7.
23. Song F, Shen X, Xiang J, Zhu Y. Characterization and magnetic properties of $Ba_xSr_{1-x}Fe_{12}O_{19}$ ($x = 0$–1) ferrite hollow fibers via gel-precursor transformation process. *J Alloys Compd* 2010;**507**:297–301.
24. Song F, Shen X, Xiang J, Song H. Formation and magnetic properties of M-Sr ferrite hollow fibers via organic gel-precursor transformation process. *Mater Chem Phys* 2010;**120**:213–6.
25. Pullar RC, Bhattacharya AK. Crystallisation of hexagonal M ferrites from a stoichiometric sol–gel precursor, without formation of the α-$BaFe_2O_4$ intermediate phase. *Mater Lett* 2002;**57**:537–42.
26. Pullar RC. A method for the preparation of aligned fibre samples for magnetic measurement using VSM. *J Magn Magn Mater* 2000;**218**:1–4.
27. Pullar RC, Bhattacharya AK. Magnetic properties of aligned M hexa-ferrite fibres. *J Magn Magn Mater* 2006;**300**:490–9.
28. Kojima H. In: Wohlfarth EP, editor. *Ferromagnetic materials*, vol. 3. Amsterdam: North-Holland Physics Publishing; 1982. pp. 305–391.
29. Shirk BT, Buessem WR. Temperature dependence of M_s and K_1 of $BaFe_{12}O_{19}$ and $SrFe_{12}O_{19}$ single crystals. *J Appl Phys* 1969;**40**:1294–6.
30. (a) Lotgering FK. Topotactical reactions with ferrimagnetic oxides having hexagonal crystal structures-I. *J Inorg Nucl Chem* 1959;**9**:113–23;
(b) Lotgering FK. Topotactical reactions with ferrimagnetic oxides having hexagonal crystal structures-II. *J Inorg Nucl Chem* 1960;**16**:100–8.
31. Gao D, Shi Z, Xu Y, Zhang J, Yang G, Zhang J, et al. Synthesis, magnetic anisotropy and optical properties of preferred oriented zinc ferrite nanowire arrays. *Nanoscale Res Lett* 2010;**5**:1289–94.